^{18}F-FDG PET and MR Imaging Associations Across a Spectrum of Pediatric Brain Tumors: A Report from the Pediatric Brain Tumor Consortium

Katherine Zukotynski[1,2], Frederic Fahey[2,3], Mehmet Kocak[4], Larry Kun[5], James Boyett[6], Maryam Fouladi[7], Sridhar Vajapeyam[2,3], Ted Treves[2,3], and Tina Y. Poussaint[2,3]

[1]Department of Medical Imaging, Sunnybrook Health Sciences Centre, University of Toronto, Ontario, Canada; [2]Department of Radiology, Harvard Medical School, Boston, Massachusetts; [3]Department of Radiology, Boston Children's Hospital, Boston, Massachusetts; [4]Department of Preventive Medicine, University of Tennessee Health Science Center, Memphis, Tennessee; [5]Department of Radiological Sciences, St. Jude Children's Research Hospital, Memphis, Tennessee; [6]Department of Biostatistics, St. Jude Children's Research Hospital, Memphis, Tennessee; and [7]Department of Hematology/Oncology, Cincinnati Children's Medical Center, Cincinnati, Ohio

The purpose of this study was to describe ^{18}F-FDG uptake across a spectrum of pediatric brain tumors and correlate ^{18}F-FDG PET with MR imaging variables, progression-free survival (PFS), and overall survival (OS). **Methods:** A retrospective analysis was conducted of children enrolled in phase I/II clinical trials through the Pediatric Brain Tumor Consortium from August 2000 to June 2010. PET variables were summarized within diagnostic categories using descriptive statistics. Associations of PET with MR imaging variables and PFS and OS by tumor types were evaluated. **Results:** Baseline ^{18}F-FDG PET was available in 203 children; 66 had newly diagnosed brain tumors, and 137 had recurrent/refractory brain tumors before enrolling in a Pediatric Brain Tumor Consortium trial. MR imaging was performed within 2 wk of PET and before therapy in all cases. The ^{18}F-FDG uptake pattern and MR imaging contrast enhancement (CE) varied by tumor type. On average, glioblastoma multiforme and medulloblastoma had uniform, intense uptake throughout the tumor, whereas brain stem gliomas (BSGs) had low uptake in less than 50% of the tumor and ependymoma had low uptake throughout the tumor. For newly diagnosed BSG, correlation of ^{18}F-FDG uptake with CE portended reduced OS (P = 0.032); in refractory/recurrent BSG, lack of correlation between ^{18}F-FDG uptake and CE suggested decreased PFS (P = 0.023). In newly diagnosed BSG for which more than 50% of the tumor had ^{18}F-FDG uptake, there was a suggestion of lower apparent diffusion coefficient (P = 0.061) and decreased PFS (P = 0.065). **Conclusion:** ^{18}F-FDG PET and MR imaging showed a spectrum of patterns depending on tumor type. In newly diagnosed BSG, the correlation of ^{18}F-FDG uptake and CE suggested decreased OS, likely related to more aggressive disease. When more than 50% of the tumor had ^{18}F-FDG uptake, the apparent diffusion coefficient was lower, consistent with increased cellularity. In refractory/recurrent BSG, poor correlation between ^{18}F-FDG uptake and CE was associated with decreased PFS, which may reflect concurrent tissue breakdown at sites of treated disease and development of new sites of ^{18}F-FDG–avid malignancy.

Received Feb. 24, 2014; revision accepted Jun. 26, 2014.
For correspondence or reprints contact: Tina Young Poussaint, Department of Radiology, Boston Children's Hospital, 300 Longwood Ave., Boston, MA 02115.
E-mail: tinayoung.poussaint@childrens.harvard.edu
Published online Jul. 28, 2014.

Key Words: MR diffusion; ^{18}F-FDG PET; pediatric; brain tumor

J Nucl Med 2014; 55:1473–1480
DOI: 10.2967/jnumed.114.139626

Brain tumors are the most common solid tumors (*1*) and second leading cause of cancer death in children (*2*). Classified by cell type and histologically graded using World Health Organization criteria (*3*), prognosis differs depending on histology, location, extent, and molecular subtypes (*4*). The Pediatric Brain Tumor Consortium (PBTC) was formed to conduct phase I/II clinical trials for children with primary brain tumors, characterize reliable biomarkers and predictors of therapy response, and develop and coordinate innovative neuroimaging techniques (*5*).

^{18}F-FDG PET is helpful in evaluating pediatric brain tumors for which ^{18}F-FDG uptake intensity and uniformity have been linked with tumor type, malignancy grade, and prognosis (*6–13*). Combining ^{18}F-FDG PET and MR imaging allows for metabolic and anatomic evaluation of pediatric brain tumors (*14,15*). A better understanding of variations in ^{18}F-FDG PET and MR imaging findings across the spectrum of pediatric tumors may clarify early markers of therapy response and survival, ultimately improving clinical management. Our aim was to describe patterns of tumor ^{18}F-FDG uptake and correlate ^{18}F-FDG PET with MR imaging variables, progression-free survival (PFS), and overall survival (OS).

MATERIALS AND METHODS

A retrospective analysis was conducted of all children with 1 baseline-interpretable ^{18}F-FDG PET scan, enrolled in a PBTC phase I/II trial from August 2000 to June 2010. All children underwent pretherapy MR imaging within 2 wk of PET. The institutional review boards of all sites approved each trial before patient enrollment, and approval was maintained throughout the studies. MR and ^{18}F-FDG PET imaging data acquired at participating institutions were electronically transferred to the PBTC Operations and Biostatistics Center and PBTC Neuroimaging Center for analysis (*16*). Investigators at the Neuroimaging Center were masked to patient outcome at the time of image evaluation.

^{18}F-FDG PET and MR Imaging Acquisition

^{18}F-FDG PET was performed using a variety of scanners (AdvanceNXI, DiscoveryLS, and DiscoverySTE [GE Healthcare]; G-PET [Philips]; HR1 and HiRez Bioscan [Siemens]). Consistency was maintained by adherence to a standard acquisition protocol and quality assurance program including daily blank scans, quarterly normalization, calibration, and preventive maintenance (*17*). Patients fasted for 4 h before ^{18}F-FDG administration. Baseline brain PET was acquired in 3-dimensional mode for 10 min, 40–60 min after intravenous administration of ^{18}F-FDG (5.55 MBq/kg; minimum, 18 MBq; maximum, 370 MBq). Attenuation correction was performed using a 3-min segmented transmission scan with ^{68}Ge/^{68}Ga rods for PET-only scanners or a CT-based approach with PET/CT scanners. Data were reconstructed using Fourier rebinning, followed by a 2-dimensional ordered-subset expectation maximization reconstruction algorithm.

MR imaging was performed at each institution using 1.5-T scanners with axial T1, fluid-attenuated inversion recovery (FLAIR), and T2 sequences. T1 images were also acquired after gadolinium diethylenetriamine pentaacetic acid (Gd-DTPA) contrast administration. Gd-DTPA axial T1–weighted spin-echo images were 4-mm contiguous slices using a repetition time (TR)/echo time (TE) of 500–700 ms/minimum full. FLAIR images were 4-mm contiguous slices using a TR/time of inversion/TE of 10,000/2,200/162 ms. Diffusion images were single-shot echoplanar spin-echo images with a TR/TE of 2,000/80 ms, 128 × 128 matrix, b-factor of 5/1,000s/mm^2, 3 directions (*x,y,z*) for trace imaging, receiver bandwidth of ±64kHz, frequency direction right to left (R/L), and slice thickness/gap of 4/0.

Image Analysis

Tumor extent was evaluated by a pediatric neuroradiologist using axial T1 post–Gd-DTPA, FLAIR, and T2-weighted MR imaging. Apparent diffusion coefficient (ADC) image/region-of-interest (ROI) analyses were performed using ImageJ (U.S. National Institutes of Health). From the ADC map, an ROI (diameter, 3–5 mm) within the solid part of the tumor was determined using T1, FLAIR, T2, and post–Gd-DTPA T1 as a reference. The mean ADC of the ROI was divided by the mean ADC from an ROI in normal frontal white matter (WM) to obtain the normalized ADC within the tumor.

^{18}F-FDG PET and MR imaging data were registered using a mutual-information algorithm. The registration quality was evaluated subjectively, and the data were analyzed by consensus among a neuroradiologist, nuclear medicine physician, and nuclear medicine physicist (*11,15*). The data analysis has been previously described (*14*). ^{18}F-FDG uptake uniformity was subjectively graded as percentage of tumor (on FLAIR) demonstrating ^{18}F-FDG uptake using a 4-point scale (0, <25%; 1, 26%–50%; 2, 51%–75%; and 3, 76%–100%) reached as a consensus between the neuroradiologist and the PET experts. ^{18}F-FDG uptake intensity was subjectively categorized using a 5-point scale (1, <WM; 2, similar to WM; 3, >WM but <gray matter [GM]; 4, similar to GM; and 5, >GM). Grade 0 uniformity indicated negligible tumor ^{18}F-FDG uptake. The axial image through the tumor containing the highest ^{18}F-FDG uptake was identified, and a 2-dimensional ROI was manually drawn based on tumor ^{18}F-FDG definition. Because of the wide range of ^{18}F-FDG uptake across all tumor types, a set threshold could not be used and ROIs were defined subjectively. Because PET data were from a multicenter trial, ROI values were standardized by normalizing values by a comparison region (contralateral WM or GM) as previously reported (*14*). Continuous PET variables including mean or maximum tumor ^{18}F-FDG uptake normalized by WM or GM were derived.

Linear associations between continuous variables of interest were described using the Spearman rank correlation coefficient, and χ^2 (or Armitage Trend tests, when appropriate) was used to describe the association between categoric variables of interest. To compare the distribution of a continuous imaging marker between 2 groups of patients, the Wilcoxon–Mann–Whitney test was used. Distributions of PFS and OS were estimated using the Kaplan–Meier method, and survival distributions were compared between 2 or more groups using the log-rank test. Cox proportional hazards models were used to investigate associations of continuous ^{18}F-FDG PET variables, PFS, and OS. OS was defined as the interval between initiation of treatment and death on study. PFS was defined as the interval between initiation of treatment and the earliest of either progressive disease or death during the study for patients whose treatment failed. Patients without failure for PFS or OS were censored at the off-study date. When statistically appropriate, log-transformation of covariates was used in survival models.

RESULTS

An interpretable baseline ^{18}F-FDG PET scan was available in 203 children (104 girls, 99 boys; age, 0.4–21 y): 66 newly diagnosed (ND) brain tumors and 137 refractory/recurrent (RR) disease (Table 1) enrolled in a PBTC phase I/II trial between

TABLE 1
Pediatric Brain Tumor Types with Baseline ^{18}F-FDG PET

Diagnosis	ND			RR		
	No. of patients	Death	Progression	No. of patients	Death	Progression
BSG	53	46	50	18	8	15
GBM	9	7	9	15	6	14
Anaplastic astrocytoma	2	1	2	28	10	24
Astrocytoma/astrocytic glioma	—	—	—	23	3	15
Ependymoma	—	—	—	15	2	12
Medulloblastoma	—	—	—	10	0	7
Primitive neuroectodermal tumor/ pineoblastoma	—	—	—	5	3	5
Others*	2	2	2	23	5	14

*Others: anaplastic ganglioglioma, ganglioglioma, glioblastoma (NOS), malignant glioma, malignant glioma (NOS except nasal glioma, not neoplastic), gliomatosis cerebri, gliosarcoma, mixed oligoastrocytoma, myxopapillary ependymoma, pleomorphic xanthoastrocytoma, rhabdoid sarcoma.

TABLE 2
^{18}F-FDG Uptake Intensity by Tumor Type

Tumor type	^{18}F-FDG uptake intensity										
	<WM (no further data)		Similar to WM		>WM and <GM		Similar to GM		>GM		
	n	Row %	*n*	Row %	*n*	Row %	*n*	Row %	*n*	Row %	All patients (*n*)
Anaplastic astrocytoma RR	3	10.7	3	10.7	10	35.7	4	14.3	8	28.6	28
Astrocytoma/astrocytic glioma RR	3	13.0	4	17.4	5	21.7	7	30.4	4	17.4	23
Ependymoma RR	6	40.0	2	13.3	6	40.0	1	6.7	—	—	15
Medulloblastoma RR	2	20.0	—	—	3	30.0	1	10.0	4	40.0	10
BSG ND	8	15.1	7	13.2	29	54.7	3	5.7	6	11.3	53
BSG RR (P = 0.40)*	2	11.1	1	5.6	14	77.8	1	5.6	—	—	18
GBM ND	1	11.1	.	—	2	22.2	2	22.2	4	44.4	9
GBM RR (P = 0.76)*	—	—	1	6.7	5	33.3	4	26.7	5	33.3	15
All patients	25	14.6	18	10.5	74	43.3	23	13.5	31	18.1	171

*Comparing ND with RR patients using Cochran–Armitage Trend test.
Data for ND (anaplastic astrocytoma, primitive neuroectodermal tumor/pineoblastoma, and other categories) and for RR (primitive neuroectodermal tumor/pineoblastoma, and other categories) in Table 1 have not been included because of small sample size. Column categories are based on subjective grading of intensity of ^{18}F-FDG uptake.

August 2000 and June 2010. Baseline MR imaging was performed within 2 wk of baseline PET in all cases. Astrocytoma included juvenile astrocytoma, pilocytic astrocytoma, and astrocytoma not otherwise specified (NOS); medulloblastoma included desmoplastic medulloblastoma and medulloblastoma NOS; and ependymoma included anaplastic ependymoma and ependymoma NOS.

PET Variables

The intensity and uniformity of ^{18}F-FDG uptake varied by brain tumor type. Because of the small sample size, analysis was possible only for a subgroup of types (Tables 2–4). In Table 2, the column categories are based on subjective ^{18}F-FDG uptake grading.

ND brain stem gliomas (BSGs) (Fig. 1A) typically had ^{18}F-FDG uptake intensity between WM and GM in <25% to >75% of the tumor, whereas RR BSGs (Fig. 1B) had ^{18}F-FDG uptake intensity between WM and GM in <25% of the tumor. There was no significant difference between ^{18}F-FDG uptake intensity and uniformity in ND versus RR BSG (P = 0.40 and 0.10, respectively). There was the suggestion that a small subpopulation of ND

TABLE 3
^{18}F-FDG Uptake Uniformity by Tumor Type

Tumor type	Uniformity								
	<25%		25%–50%		51%–75%		76%–100%		
	n	Row %	*n*	Row %	*n*	Row %	*n*	Row %	All patients (*n*)
Anaplastic astrocytoma RR	9	36.0	7	28.0	4	16.0	5	20.0	25
Astrocytoma/astrocytic glioma RR	1	5.3	1	5.3	6	31.6	11	57.9	19
Ependymoma RR	2	25.0	1	12.5	1	12.5	4	50.0	8
Medulloblastoma RR	—	—	—	—	1	12.5	7	87.5	8
BSG ND	12	26.7	12	26.7	6	13.3	15	33.3	45
BSG RR (P = 0.10)*	9	56.3	2	12.5	3	18.8	2	12.5	16
GBM ND	2	25.0	1	12.5	1	12.5	4	50.0	8
GBM RR (P = 0.91)*	2	13.3	4	26.7	3	20.0	6	40.0	15
All patients	37	25.7	28	19.4	25	17.4	54	37.5	144†

*ND vs. RR compared using Cochran–Armitage Trend test.
†Uniformity data missing for 27 patients.

TABLE 4
Descriptive Statistics of Continuous PET Variables by Tumor Types

Tumor type	*n*	Minimum	Median	Maximum	*P**
Mean tumor ^{18}F-FDG uptake/GM					
Anaplastic astrocytoma RR	25	0.38	0.85	2.35	
Astrocytoma/astrocytic glioma RR	20	0.35	0.70	2.68	
BSG RR	16	0.13	0.49	0.88	0.067
BSG ND	45	0.38	0.61	1.23	
Ependymoma RR	9	0.48	0.59	0.80	
GBM RR	15	0.55	0.68	2.59	0.23
GBM ND	8	0.55	1.02	1.45	
Medulloblastoma RR	8	0.62	0.84	1.29	
Maximum tumor ^{18}F-FDG uptake/GM					
Anaplastic astrocytoma RR	25	0.45	0.97	3.44	
Astrocytoma/astrocytic glioma RR	20	0.41	0.81	3.69	
BSG RR	16	0.33	0.51	0.90	0.053
BSG ND	45	0.38	0.63	1.48	
Ependymoma RR	9	0.48	0.65	0.84	
GBM RR	15	0.60	0.80	3.14	0.25
GBM ND	8	0.72	1.15	2.50	
Medulloblastoma RR	8	0.63	0.92	1.37	
Mean tumor ^{18}F-FDG uptake/WM					
Anaplastic astrocytoma RR	25	0.82	1.42	3.15	
Astrocytoma/astrocytic glioma RR	20	0.87	1.70	4.37	
BSG RR	16	0.97	1.18	1.71	0.23
BSG ND	45	0.71	1.28	2.89	
Ependymoma RR	9	0.85	1.59	2.43	
GBM RR	15	1.26	1.55	6.36	0.042
GBM ND	8	1.51	2.93	5.77	
Medulloblastoma RR	8	1.18	2.40	3.91	
Maximum tumor ^{18}F-FDG uptake/WM					
Anaplastic astrocytoma RR	25	0.77	1.54	6.45	
Astrocytoma/astrocytic glioma RR	20	0.81	1.75	5.47	
BSG RR	16	0.63	1.07	1.65	0.26
BSG ND	45	0.67	1.23	2.85	
Ependymoma RR	9	0.89	1.42	2.25	
GBM RR	15	1.00	1.55	7.17	0.032
GBM ND	8	1.36	2.92	8.76	
Medulloblastoma RR	8	1.27	2.04	4.18	

*P value is from Wilcoxon–Mann–Whitney test comparing ND vs. RR.

BSG had intense or uniform ^{18}F-FDG uptake, whereas this was rare in RR BSG. In ND BSG, if ^{18}F-FDG uptake intensity was similar to or >GM (~10% of cases), ^{18}F-FDG uptake was often spread throughout >50% of the tumor (~80% of cases). If ^{18}F-FDG uptake intensity was <GM, ^{18}F-FDG uptake was seen in 50% or less of the tumor (P = 0.06). There was no significant relationship between ^{18}F-FDG uptake intensity and uniformity in RR BSG (P = 1.0).

ND glioblastoma multiforme (GBM) (Fig. 2A) often had ^{18}F-FDG uptake intensity similar to or >GM in >75% of the tumor, whereas RR GBM (Fig. 2B) often had ^{18}F-FDG uptake intensity similar to or >GM in >50% of the tumor. There was no significant difference between ^{18}F-FDG uptake intensity or uniformity in ND versus RR GBM (P = 0.76 and 0.91, respectively) and no significant relationship between ^{18}F-FDG uptake intensity and uniformity in RR GBM (P = 1.0).

RR medulloblastoma typically had intense, diffuse ^{18}F-FDG uptake throughout the tumor (Fig. 3A), whereas RR anaplastic astrocytoma had mild-moderate ^{18}F-FDG uptake in a smaller amount of the tumor (Fig. 3B). In RR astrocytoma/astrocytic

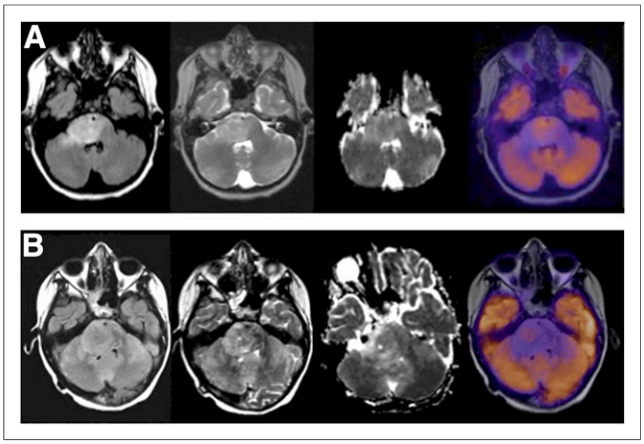

FIGURE 1. ^{18}F-FDG uptake intensity and uniformity in BSG. (A) An 11-y-old boy with ND BSG showing intensity of ^{18}F-FDG uptake between WM and GM in 50%–75% of tumor as defined on FLAIR. From left to right are FLAIR, T2, ADC, and PET images. In region of uptake within BSG there is lower ADC value. (B) An 8-y-old girl with RR BSG showing intensity of ^{18}F-FDG uptake between WM and GM in <25% of tumor (FLAIR). From left to right are FLAIR, T2, ADC, and PET images.

glioma, the appearance was often mild-moderate ^{18}F-FDG uptake in most of the tumor (Fig. 3C). There was no significant relationship between ^{18}F-FDG uptake intensity and uniformity in RR anaplastic astrocytoma or astrocytoma/astrocytic glioma. ^{18}F-FDG uptake in ependymoma was often mild and spread throughout the tumor (Fig. 3D). More than half the children had tumor ^{18}F-FDG uptake similar to or <WM, whereas this was less than a third in almost all other tumor types.

Median maximum tumor ^{18}F-FDG uptake/GM was highest in ND GBM, followed by RR: anaplastic astrocytoma, medulloblastoma, astrocytoma/astrocytic glioma, GBM and ependymoma, and finally ND and RR BSG. Median maximum tumor ^{18}F-FDG uptake/WM was highest in ND GBM, followed by RR: medulloblastoma, astrocytoma/astrocytic glioma, GBM, anaplastic astrocytoma, and ependymoma, and finally ND and RR BSG. ND GBM had higher mean and maximum tumor ^{18}F-FDG uptake/WM than RR GBM ($P = 0.042$ and 0.032, respectively), suggesting ND BSG had higher mean and maximum tumor ^{18}F-FDG uptake/GM than RR BSG ($P = 0.067$ and 0.053, respectively). When ND and RR cohorts were combined, GBM had higher tumor ^{18}F-FDG uptake–to–comparative tissue ratios ($P < 0.001$) than BSG.

PET and MR Imaging Variable Correlation

Evaluation of both tumor MR imaging contrast enhancement (CE) and PET ^{18}F-FDG uptake was possible in 120 children (Supplemental Table 1; supplemental materials are available at http://jnm.snmjournals.org). Near-complete or complete correlation was most common in GBM and medulloblastoma and least common in BSG and anaplastic astrocytoma. There was no significant difference in correlation of CE and ^{18}F-FDG uptake between ND and RR BSG ($P = 0.75$), although GBM had higher correlation of CE with ^{18}F-FDG uptake than BSG ($P = 0.0011$).

In ND BSG, intense ^{18}F-FDG uptake (uptake similar to or >GM) suggested lower ADC ($P = 0.075$), and uniform ^{18}F-FDG uptake (uptake in >50% of tumor) suggested lower ADC ($P = 0.061$). In general, ND BSG had less CE ($P < 0.0001$) and higher ADC ($P = 0.03$) than RR BSG.

In ND BSG (Supplemental Table 2), maximum tumor ^{18}F-FDG uptake/WM correlated with ADC. Mean tumor ^{18}F-FDG uptake/WM correlated with CE and ADC. In RR GBM, there was correlation of maximum tumor ^{18}F-FDG uptake/GM, mean tumor ^{18}F-FDG uptake/GM, maximum tumor ^{18}F-FDG uptake/WM, and mean tumor ^{18}F-FDG uptake/WM with CE.

In ND BSG, there was a suggestion that ^{18}F-FDG uptake in >50% of the tumor was associated with decreased PFS ($P = 0.065$), although not with OS ($P = 0.17$). There was no association of ^{18}F-FDG uptake intensity with PFS or OS (Supplemental Table 3).

In RR BSG, GBM, and astrocytoma, there was no association of ^{18}F-FDG uptake uniformity or intensity with survival. There was correlation of mean tumor ^{18}F-FDG uptake/GM with OS for anaplastic astrocytoma ($P = 0.014$).

In ND BSG, higher correlation of MR imaging CE and PET ^{18}F-FDG uptake was not associated with PFS ($P = 0.7$) but suggested worse OS ($P = 0.032$) (Figs. 4A and 4B). In RR BSG, increased CE suggested lower PFS ($P = 0.0081$, Supplemental Table 3), and higher correlation of MR imaging CE and PET ^{18}F-FDG uptake suggested more favorable PFS ($P = 0.023$) but was not associated with OS ($P = 0.25$) (Figs. 4C and 4D). The association between correlation of MR imaging CE and PET ^{18}F-FDG uptake intensity and uniformity with PFS and OS could not be calculated for other tumor types given the small sample size.

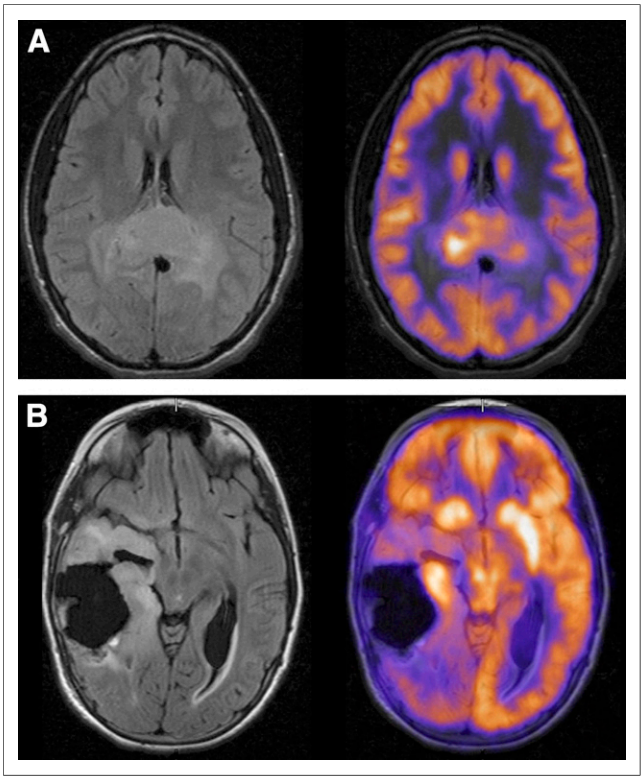

FIGURE 2. ^{18}F-FDG uptake intensity and uniformity in GBM. (A) An 18-y-old boy with ND GBM showing intensity of ^{18}F-FDG uptake similar to GM in >75% of tumor (FLAIR). (B) An 11-y-old girl with RR GBM showing intensity of ^{18}F-FDG uptake >GM in <25% of tumor (FLAIR).

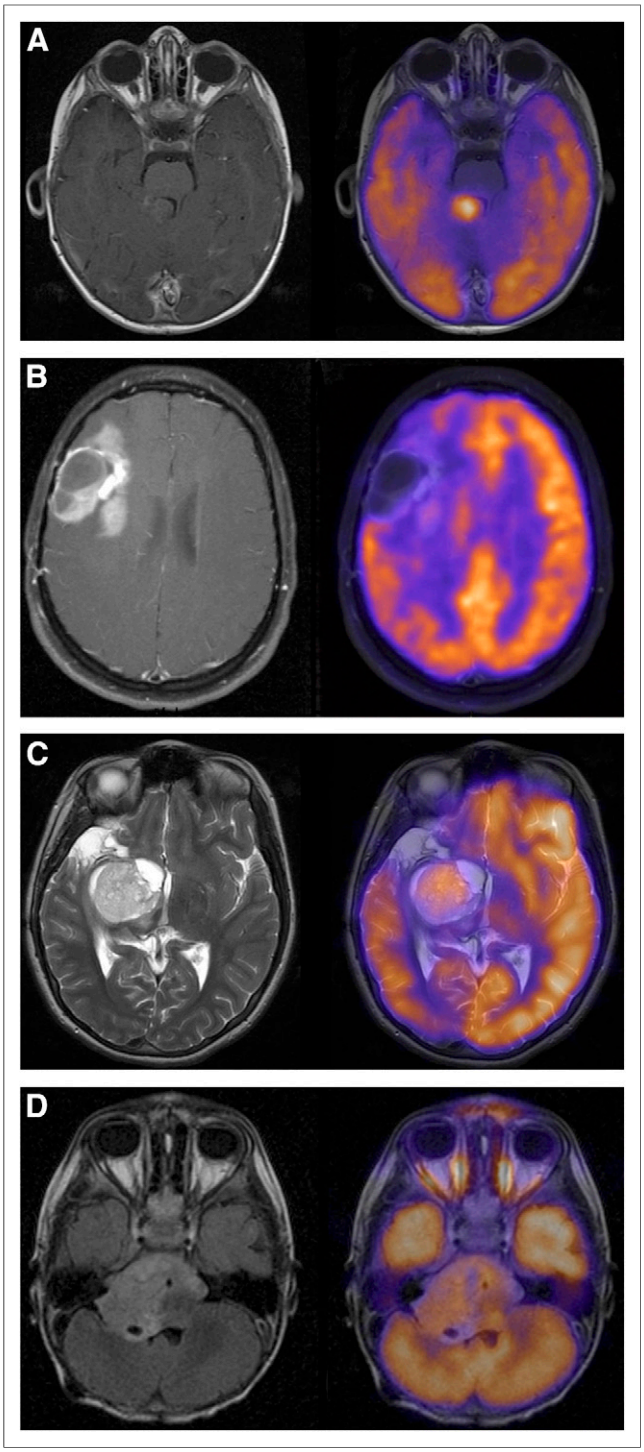

FIGURE 3. ^{18}F-FDG uptake intensity and uniformity in medulloblastoma, anaplastic astrocytoma, astrocytoma, and ependymoma. (A) A 22-mo-old boy with RR medulloblastoma showing intensity of ^{18}F-FDG uptake >GM in >75% of tumor (T1 post–Gd-DTPA). (B) A 15-y-old girl with RR anaplastic astrocytoma showing intensity of ^{18}F-FDG uptake between WM and GM in 50%–75% of tumor (T1 post–Gd-DTPA). (C) A 15-y-old girl with RR astrocytoma showing intensity of ^{18}F-FDG uptake similar to GM in >75% of tumor (T2). (D) A 2-y-old boy with RR ependymoma showing intensity of ^{18}F-FDG uptake between WM and GM in >75% of tumor (FLAIR).

DISCUSSION

^{18}F-FDG PET and MR imaging provide complementary evaluation of pediatric brain tumors. Kwon et al. (*6*) studied 20 children with BSG and stereotactic biopsy or surgery. Twelve underwent preoperative ^{18}F-FDG PET and MR imaging. The authors concluded that metabolism on ^{18}F-FDG PET and enhancement on MR imaging differed by histology and were complementary. Borgwardt et al. (*7*) evaluated 38 children with a spectrum of primary brain tumors, pretherapy ^{18}F-FDG PET, and MR imaging. They found improved tumor characterization when PET and MR imaging were coregistered. Also ^{18}F-FDG uptake positively correlated with malignancy grade.

There is evidence suggesting that ^{18}F-FDG uptake is associated with histologic grade and provides prognostic information in the pediatric population. Hoffman et al. (*8*) reviewed ^{18}F-FDG PET in 17 children with posterior fossa tumors and found that increased uptake suggested more aggressive tumor types. Holthoff et al. (*9*) studied ^{18}F-FDG PET in 15 children and found increased ^{18}F-FDG uptake in medulloblastoma, compared with other posterior fossa tumors. Williams et al. (*11*) showed 3-dimensional maximum and mean tumor ^{18}F-FDG uptake was associated with PFS in pediatric supratentorial anaplastic astrocytomas. Gururangan et al. (*18*) found a significant negative correlation between ^{18}F-FDG uptake and survival in 22 children with ND or recurrent medulloblastoma. Kruer et al. (*13*) reported ^{18}F-FDG PET was an independent measure of disease risk stratification in 46 children with low-grade astrocytomas.

There is the suggestion that ^{18}F-FDG PET improves management of pediatric brain tumors. Pirotte et al. (*12*) reviewed ^{18}F-FDG PET in 20 children. Higher tumor ^{18}F-FDG uptake suggested higher grade and shorter survival. PET guidance improved diagnostic yield at biopsy, compared with MR imaging. Pirotte et al. (*19*) also suggested that ^{18}F-FDG PET helps differentiate indolent from active disease; improves lesion delineation, compared with MR imaging; and impacts intervention.

The association of ^{18}F-FDG PET and MR imaging in pediatric brain tumors provides both metabolic and anatomic information. In our review of 40 children with ND BSG, when tumor ^{18}F-FDG uptake uniformity was higher, ADC was lower, suggesting an increased number of metabolically viable tumor cells associated with increased tumor cellularity and restricted ADC (*14*). We also found that higher ^{18}F-FDG uptake suggested increased tumor CE and hypothesized this could be due to more aggressive disease because most BSGs do not enhance (*20*). In a subsequent exploratory evaluation, we suggested that the correlation of tumor ^{18}F-FDG uptake on PET with MR CE and perfusion metrics provides a more complete understanding of tumor biology and aggressiveness (*15*).

In this study, ^{18}F-FDG PET and MR imaging associations were evaluated across a spectrum of pediatric brain tumors. Hypermetabolic tumor types were typically GBM, anaplastic astrocytoma, and medulloblastoma whereas BSG and ependymoma tended to be less ^{18}F-FDG–avid. ^{18}F-FDG uptake was commonly intense and uniform in GBM and medulloblastoma, consistent with often aggressive, locally invasive, extensive disease. Low-grade lesions such as pilocytic astrocytoma can be hypermetabolic, contrary to the supposition that high uptake dictates aggressiveness (*21,22*).

A subset of children with ND BSG had intense, uniform ^{18}F-FDG uptake, although most had ^{18}F-FDG uptake between WM and GM in <50% of the tumor. Also in ND BSG, intense or uniform ^{18}F-FDG uptake suggested increased MR CE and lower

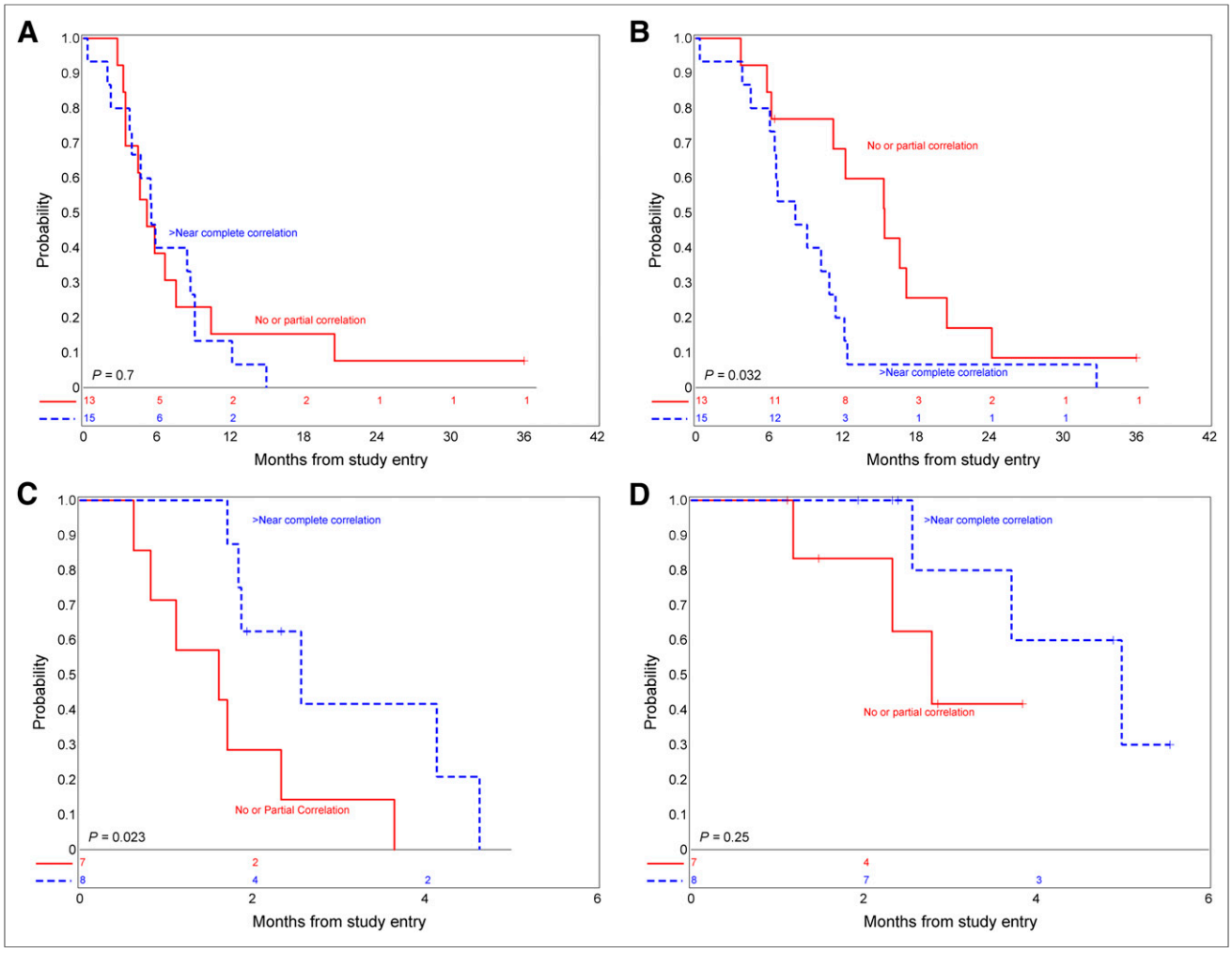

FIGURE 4. (A) Association between PFS and CE in ND BSG. (B) Association between OS and CE in ND BSG. (C) Association between PFS and CE in RR BSG. (D) Association between OS and CE in RR BSG.

ADC, possibly reflecting a subset of aggressive baseline pediatric BSG with increased viable cellularity. ND BSG had less CE and higher ADC than RR BSG. Without a biopsy, the histologic milieu is unknown; however, BSGs at baseline often have increased ADC likely due to a combination of low tumor cellularity and vasogenic edema (*23*).

BSG was the only tumor type for which a statistical analysis correlating ^{18}F-FDG uptake with MR CE and survival (PFS and OS) could be performed for both ND and RR disease. We found a suggestive association of ^{18}F-FDG uptake uniformity with PFS similar to prior results; however, given the heterogeneity of ^{18}F-FDG uptake across all children with BSG, the small sample size, and the dismal prognosis, a statistically meaningful correlation of ^{18}F-FDG uptake pattern with PFS and OS was not reached. A larger prospective study is needed to verify the hypothesis that ^{18}F-FDG uptake pattern predicts survival. Also, in ND BSG, correlation of tumor CE and ^{18}F-FDG uptake suggested worse OS ($P = 0.032$), whereas in RR BSG, correlation of CE and ^{18}F-FDG uptake suggested more favorable PFS ($P = 0.023$). Thus, correlation of ^{18}F-FDG uptake and CE in pediatric BSG at baseline suggests decreased survival, likely related to more aggressive disease. After therapy, this relationship is reversed, possibly reflecting decreased survival with development of new sites of ^{18}F-FDG–avid malignancy.

The main limitations of this study are small sample size and poor survival, making it difficult to draw statistically meaningful inferences. Our sample size, however, is significantly larger than previously published studies and will contribute to the growing literature on ^{18}F-FDG PET and MR imaging associations across the spectrum of pediatric brain tumors. The study was also performed on a variety of tumor types over a span of almost a decade. For this analysis, it was decided to use a consistent approach to image analysis involving the manual definition of a 2-dimensional ROI based on ^{18}F-FDG uptake. Future analyses of similar data may involve an automated 3-dimensional voxel-based approach. In the correlation of MR and ^{18}F-FDG PET, the ROIs on the 2 studies were defined independently and, thus, may not have coincided. The correlation of areas of highest signal for each modality is a reasonable approach, although we have also investigated the use of a common ROI in these analyses (*15*). Future studies could evaluate PET/MR or additional PET radiopharmaceuticals such as ^{18}F-fluorothymidine, ^{18}F-fluoroazomycin arabinoside, or ^{18}F-fluoroethyl-L-tyrosine in pediatric brain tumors. PET/MR has the potential for simultaneous acquisition of PET and MR imaging with real-time metabolic and anatomic image registration on a voxel-by-voxel basis. Further, PET/MR would likely require a single visit to the imaging department, improving

convenience with lower radiation exposure than is needed for PET/CT plus MR imaging. Finally, novel PET tracers may result in improved sensitivity or insight into tumor biology by studying aspects of proliferation and hypoxia.

CONCLUSION

^{18}F-FDG PET uptake patterns vary depending on pediatric brain tumor type, with GBM and medulloblastoma commonly showing uniformly hypermetabolic disease, whereas BSG and ependymoma are not significantly ^{18}F-FDG–avid. At baseline, NG BSGs often have less CE and increased ADC, suggesting decreased baseline aggressiveness and cellularity. Although the correlation of ^{18}F-FDG uptake and CE in ND BSG suggests decreased survival, after therapy this relationship is reversed, likely reflecting poor survival in children with concurrent blood–brain barrier breakdown at sites of treated disease and development of new sites of ^{18}F-FDG–avid malignancy.

DISCLOSURE

The costs of publication of this article were defrayed in part by the payment of page charges. Therefore, and solely to indicate this fact, this article is hereby marked "advertisement" in accordance with 18 USC section 1734. This study was supported by NIH grant U01 CA81457 for the Pediatric Brain Tumor Consortium (PBTC), Pediatric Brain Tumor Consortium Foundation (PBTCF), Pediatric Brain Tumor Foundation of the United States (PBTFUS), and American Lebanese Syrian Associated Charities (ALSAC). No other potential conflict of interest relevant to this article was reported.

ACKNOWLEDGMENT

We acknowledge Cynthia Dubé for help with manuscript preparation.

REFERENCES

1. National Cancer Institute. National Cancer Institute fact sheet: childhood cancers. NCI website. http://www.cancer.gov/cancertopics/factsheet/Sites-Types/childhood. June 2008. Accessed July 5, 2014.
2. American Brain Tumor Association. Brain tumor statistics. ABTA website. http://www.abta.org/news/brain-tumor-fact-sheets/. Accessed July 5, 2014.
3. Louis DN, Ohgaki H, Wiestler OD, et al. The 2007 WHO classification of tumours of the central nervous system. *Acta Neuropathol.* 2007;114:97–109.
4. Taylor MD, Northcott PA, Korshunov A, et al. Molecular subgroups of medulloblastoma: the current consensus. *Acta Neuropathol.* 2012;123:465–472.
5. Pediatric Brain Tumor Consortium. Introduction to PBTC. PBTC website. http://www.pbtc.org/public/gen_info.htm. Accessed July 5, 2014.
6. Kwon JW, Kim I, Cheon J, et al. Paediatric brainstem gliomas: MRI, ^{18}F-FDG-PET and histological grading correlation. *Pediatr Radiol.* 2006;36:959–964.
7. Borgwardt L, Højgaard L, Carstensen H, et al. Increased fluorine-18 2-fluoro-2-deoxy-D-glucose (FDG) uptake in childhood CNS tumors is correlated with malignancy grade: a study with FDG positron emission tomography/magnetic resonance imaging coregistration and image fusion. *J Clin Oncol.* 2005;23:3030–3037.
8. Hoffman JM, Hanson MW, Friedman HS, et al. FDG–PET in pediatric posterior fossa brain tumors. *J Comput Assist Tomogr.* 1992;16:62–68.
9. Holthoff VA, Herholz K, Berthold F, et al. In vivo metabolism of childhood posterior fossa tumors and primitive neuroectodermal tumors before and after treatment. *Cancer.* 1993;72:1394–1403.
10. Utriainen M, Metsahonkala L, Salmi T, et al. Metabolic characterization of childhood brain tumors comparison of ^{18}F-fluorodeoxyglucose and ^{11}C-methionine positron emission tomography. *Cancer.* 2002;95:1376–1386.
11. Williams G, Fahey F, Treves ST, et al. Exploratory evaluation of two-dimensional and three-dimensional methods of ^{18}F-FDG PET quantification in pediatric anaplastic astrocytoma: a report from the Pediatric Brain Tumor Consortium (PBTC). *Eur J Nucl Med Mol Imaging.* 2008;35:1651–1658.
12. Pirotte BJ, Lubansu A, Massager N, Wikler D, Goldman S, Levivier M. Results of positron emission tomography guidance and reassessment of the utility of and indications for stereotactic biopsy in children with infiltrative brainstem tumors. *J Neurosurg.* 2007;107(5, suppl):392–399.
13. Kruer MC, Kaplan AM, Etzl MM, et al. The value of positron emission tomography and proliferation index in predicting progression in low-grade astrocytomas of childhood. *J Neurooncol.* 2009;95:239–245.
14. Zukotynski KA, Fahey FH, Kocak M, et al. Evaluation of ^{18}F-FDG PET and MRI associations in pediatric diffuse intrinsic brain stem glioma: a report from the Pediatric Brain Tumor Consortium. *J Nucl Med.* 2011;52:188–195.
15. Zukotynski KA, Fahey FH, Vajapeyam S, et al. Exploratory evaluation of MRI permeability with ^{18}F-FDG PET mapping in pediatric brain tumors: a report from the Pediatric Brain Tumor Consortium. *J Nucl Med.* 2013;54:1237–1243.
16. Poussaint TY, Philips PC, Vajapeyam S, et al. The Neuroimaging Center of the Pediatric Brain Tumor Consortium: collaborative neuroimaging in pediatric brain tumor research—a work in progress. *AJNR.* 2007;28:603–607.
17. Fahey FH, Kinahan PE, Doot RK, et al. Variability in PET quantitation within a multicenter consortium. *Med Phys.* 2010;37:3660–3666.
18. Gururangan S, Hwang E, Herendon JE II, Fuchs H, George T, Coleman RE. [^{18}F] fluorodeoxyglucose-positron emission tomography in patients with medulloblastoma. *Neurosurgery.* 2004;55:1280–1288.
19. Pirotte BJ, Lubansu A, Massager N, et al. Clinical impact of integrating positron emission tomography during surgery in 85 children with brain tumors. *J Neurosurg Pediatr.* 2010;5:486–499.
20. Fischbein NJ, Prados M, Wara W, Russo C, Edwards M, Barkovich A. Radiologic classification of brain stem tumors: correlation of magnetic resonance imaging appearance with clinical outcome. *Pediatr Neurosurg.* 1996;24:9–23.
21. Borgwardt L, Larsen HJ, Pedersen K, et al. Practical use and implementation of PET in children in a hospital PET centre. *Eur J Nucl Med Mol Imaging.* 2003;30:1389–1397.
22. Patil S, Biassoni L, Borgwardt L. Nuclear medicine in pediatric neurology and neurosurgery: epilepsy and brain tumors. *Semin Nucl Med.* 2007;37:357–381.
23. Chen HJ, Panigraphy A, Dhall G, Finlay JL, Nelson MD Jr, Blüml S. Apparent diffusion and fractional anisotropy of diffuse intrinsic brain stem gliomas. *AJNR.* 2010;31:1879–1885.

JNM The Journal of NUCLEAR MEDICINE

^{18}F-FDG PET and MR Imaging Associations Across a Spectrum of Pediatric Brain Tumors: A Report from the Pediatric Brain Tumor Consortium

Katherine Zukotynski, Frederic Fahey, Mehmet Kocak, Larry Kun, James Boyett, Maryam Fouladi, Sridhar Vajapeyam, Ted Treves and Tina Y. Poussaint

J Nucl Med. 2014;55:1473-1480.
Published online: July 28, 2014.
Doi: 10.2967/jnumed.114.139626

The Journal of Nuclear Medicine is published monthly.
SNMMI | Society of Nuclear Medicine and Molecular Imaging
1850 Samuel Morse Drive, Reston, VA 20190.
(Print ISSN: 0161-5505, Online ISSN: 2159-662X)

SNMMI SOCIETY OF NUCLEAR MEDICINE AND MOLECULAR IMAGING